The co-chaperone p23 is degraded by caspases and the proteasome during apoptosis

Jens Mollerup*, Martin W. Berchtold

Institute of Molecular Biology and Physiology, Department of Molecular Cell Biology, University of Copenhagen, Oester Farimagsgade 2A, 1353 Copenhagen K, Denmark

Received 9 May 2005; revised 23 June 2005; accepted 27 June 2005

Available online 6 July 2005

Edited by Veli-Pekka Lehto

Abstract The heat shock protein 90 co-chaperone p23 has recently been shown to be up-regulated in cancer cells and down-regulated in atheroschlerotic plaques. We found that p23 is degraded during apoptosis induced by several stimuli, including Fas and TNFα-receptor activation as well as staurosporine treatment. Caspase inhibition protected p23 from degradation in several cell lines. In addition, recombinant caspase-3 and 8 cleaved p23 at Asp 142 generating a degradation product of 18 kDa as seen in apoptotic cells. Truncated p23 is further degraded in a proteasome dependent process during apoptosis. Furthermore, we found that the anti-aggregating activity of truncated p23 was reduced compared to full length p23 indicating that caspase mediated p23 degradation contributes to protein destabilisation in apoptosis.

Keywords: Hsp90 co-chaperone; Cytosolic prostaglandin E_2 synthase; Caspase-3; Caspase-8

1. Introduction

The heat shock proteins (hsp's) are molecular chaperones that guide the folding, assembly, maturation and turnover of many key regulators of cell growth, differentiation and survival. One of the most abundant proteins in mammalian cells is hsp90 [1]. The formation of a dynamic complex with hsp90, hsp70, hsp40, heat shock organising protein (hop), p23 co-chaperone, ATP and the client protein is required for the hsp90 chaperone activity [2]. The co-chaperone p23 enters the hsp90 chaperone complex late in the maturation process of the steroid hormone receptors when hsp90 binds ATP, but no longer binds hsp70, hsp40, and hop (reviewed in [3]). p23 stimulates the ATP-driven release of the client steroid receptor protein from the chaperone complex [4].

Geldanamycin (GA) has been shown to destabilise hsp90 client proteins, leading to the demise of many oncogenic client proteins in human cancer [5]. GA and its analogues competitively inhibit ATP binding to hsp90 and prevent the ATP-dependent interaction between hsp90 and p23 [6,7]. The co-chaperone p23 has been shown to be particularly important for the hsp90 chaperone activity, because it stabilises the ATP-bound form of hsp90, and it facilitates subsequent steps in the chaperoning cycle [8]. Furthermore, p23 has been shown to be rate-limiting for hsp90 chaperone activity during glucocorticoid receptor heterocomplex formation in vitro and in vivo [9].

Hsp90 independent functions of p23 have also been found. These include passive chaperone activity [10,11] and alteration of the ligand efficiency of steroid hormone receptors [12]. Furthermore, p23 may release active steroid hormone receptors from the DNA [13]. p23 was also found to be identical to the cytoplasmic prostaglandin E_2 synthase, a glutathione dependent enzyme in the cyclooxygenase I pathway.

Recently, p23 was described to be up-regulated in rat brain ischemia, in human cancers and metastatic tissue, and to be downregulated in artherosclerotic plaques and THP-1 macrophage cells stimulated with aggregated low density lipoproteins [14–18]. Initially, we have shown that p23 is cleaved in the T cell leukemia cell line (Jurkat-E6) during Fas-induced apoptosis, indicating that p23 may be a target for proteases activated during programmed cell death [18]. In line with this finding, p23 was recently shown to be cleaved by caspases 3 and 7 following treatment of HL-60 and NB4 cell lines with GA and other chemotherapeutic drugs [19].

In this paper we report that apoptosis induced by extrinsic or intrinsic pathways lead to caspase-mediated cleavage of p23 at its C-terminal tail. This leaves a truncated p23 that has reduced passive chaperone activity. We also observed that truncated p23 is further degraded in a process dependent on proteasomal activity.

2. Materials and methods

2.1. Reagents and antibodies

The mouse anti-p23 clone 22 [18] was from BD (BD Biosciences, San Jose, FL, USA). The mouse anti-Fas antibody, clone APO-1-3, that was used to crosslink the Fas receptor in Jurkat-E6 cells, was a kind gift from Peter Krammer (Deutsches Krebsforschungszentrum, Heidelberg, Germany). The secondary goat anti-mouse immunoglobulin (Ig)-HRP and goat anti-rabbit Ig-HRP were from DakoCytomation (Glostrup, Denmark). Cycloheximide and citrate synthase (CS) were from Sigma (St. Louis, MO, USA). ^{35}S-methionine was from Perkin–Elmer (Belgium). TNT Wheat Germ Extract was from Promega Corporation (Madison, WI, USA). The purified recombinant active caspase-3 and caspase-8 were a kind gift of Henning R. Stennicke (Novo Nordisk, Bagsværd, Denmark). The recombinant human tumor necrosis factor-α (TNFα) was from Research Diagnostics Inc. (Flanders, NJ, USA). The benzyloxycarbonyl-Val-Ala-Asp-fluoromethyl ketone (zVAD-fmk) and *N*-acetyl-Asp-Glu-Val-Asp-aldehyde

*Corresponding author. Fax: +45 33935220.
E-mail address: jmollerup@my.molbio.ku.dk (J. Mollerup).

Abbreviations: hsp, heat shock protein; TNFα, tumor necrosis factor alpha; hop, heat shock organising protein; RIP, receptor interacting protein; CHIP, c-terminal of hsc70 interacting protein; CS, citrate synthase; TPR, tetratricopeptide repeat

0014-5793/$30.00 © 2005 Published by Elsevier B.V. on behalf of the Federation of European Biochemical Societies.
doi:10.1016/j.febslet.2005.06.045

(Ac-DEVD-CHO) were from Bachem AG (Bubendorf, Schwitzerland). PSI (carbobenzoxy-L-isoleucyl-γ-*t*-butyl-L-glutamyl-L-alanyl-L-leucinal) was from Affinity Bioreagents (Golden, CO, USA). GA was from Biomol Research Laboratories (Plymouth Meeting, PA, USA). All other reagents used were of analytical grade.

2.2. Cell culture and apoptosis induction

Jurkat-E6 (human T-cell leukaemia) and NIH3T3 cells were maintained in RPMI 1640 (Invitrogen Corp., Carlsbad, USA) and in DMEM (Invitrogen Corp.), respectively. Both media were supplemented with 10% heat inactivated fetal calf serum (Biochrom Ltd., Cambridge, UK), penicillin and streptomycin (Invitrogen Corp.) and cells were grown at 37 °C in a 5% CO_2 atmosphere. Apoptosis was induced in Jurkat-E6 cells by cross-linking of APO-1/CD95/Fas using the anti-APO-1-3 antibody [20] and 10 ng/ml of protein A. NIH3T3 cells were induced to apoptosis by incubation with 20 or 50 ng/ml of recombinant human TNFα, respectively, together with 10 μg/ml cycloheximide or 0.5 μM of GA. A flow cytometry based annexin-V labelling assay was primarily used to monitor apoptosis.

2.3. Cell lysates, SDS–PAGE and immunoblotting

Cells were lysed in ice-cold NP-40 lysis buffer (0.5% NP-40, 50 mM Tris, pH 7.4; 150 mM NaCl) with 0.1% protease inhibitor cocktail (Sigma, St. Louis, USA) or in RIPA lysis buffer (1% NP-40, 0.1% SDS, 0.5% Na-deoxycholate, 50 mM Tris, pH 7.4; 150 mM NaCl) with 0.1% protease inhibitor cocktail. The total protein concentrations of the cleared lysates were determined using a modified Lowry assay (Bio-Rad DC Protein Assay) with bovine serum albumin as the standard.

Before SDS–PAGE and immunoblotting, samples were diluted with lysis buffer to balance the protein concentration and then SDS sample buffer was added, followed by heating to 90 °C for 2 min. SDS–PAGE was carried out using resolving gels of 10% or 12% acrylamide with 4% stacking gel or 10–20% gradient gels (Cambrex, Bio Science Rockland, Inc., Rockland, Maine). The proteins were blotted onto Hybond-P membranes (Amersham Biosciences, Uppsala, Sweden). After blocking in Tris-buffered saline containing 5% dry skim milk and 1% Tween 20 the membranes were incubated with primary antibody for 1 h, washed three times and incubated with the secondary HRP-conjugated antibody for 1 h and finally washed as above. Immunoreactivity was visualised by chemiluminescence using ECL (Amersham Biosciences) followed by exposure to Hyperfilm (Amersham Biosciences).

2.4. Site-directed mutagenesis

Human p23 was amplified by PCR from IMAGE clone 6173097 to incorporate a Kozak sequence and restriction endonuclease sites to allow insertion in pcDNA3 (Invitrogen Corp.). The mutant constructs p23-D142E and p23-D150E were prepared by site-directed mutagenesis using the protocol of Sawano and Miyawaki [21]. Truncated p23-C18, lacking the last 18 codons, was prepared by PCR to incorporate a stop codon after D142 followed by a restriction endonuclease site. For bacterial expression of 6 × His-tagged human p23, human p23 was amplified using PCR with primer overhangs containing the 6 × His-tag and restriction sites for incorporation into a modified pGEMEX-2 vector. All p23 coding regions were verified by sequencing.

2.5. p23 cleavage by recombinant caspases

p23-wt, p23-D142E, and p23-D150E were synthesised in vitro using the TNT Coupled Wheat Germ Extract System with L-[^{35}S]-methionine incorporation from linearised DNA templates using T7 RNA polymerase. 1 μl of the ^{35}S-labelled protein was incubated with different concentrations of recombinant caspase-3 or caspase-8 in caspase buffer (20 mM PIPES, 100 mM NaCl, 10 mM DTT, 1 mM EDTA, 0.1% CHAPS, 10% sucrose, pH adjusted to 7.2) in a total volume of 20 μl, for 1 h at 37 °C. Cleavage was terminated by addition of a concentrated SDS-sample buffer (250 mM Tris, pH 8.8, 10% SDS, 0.5% bromophenol blue, 100 mM DTT, 500 mM sucrose) and incubation at 90 °C for 2 min. Samples were separated by SDS–PAGE and gels dried before autoradiography.

2.6. Citrate synthase aggregation assay by light scatter

p23 mediated inhibition of CS aggregation following heat induced inactivation at 43 °C was essentially performed as described previously [22]. Citrate synthase from porcine heart (Sigma, St. Louis, MO) was dialysed against 50 mM Tris, pH 8.0 with 2 mM EDTA. The protein concentration was determined by absorbance at 280 nm using a calculated absorption of 1.64 for a 1 mg/ml solution in a 1 cm cuvette at 280 nm. Purified 6 × His-tagged p23 protein or control proteins were added to 1500 μl of 40 mM HEPES–KOH, pH 7.5 buffer at 43 °C in a termostated cuvette with constant stirring. Light scatter at 500 nm was recorded using a spectrofluorometer (Shimadzu, Duisburg, Germany) at 5 nm slit opening. Sampling at 2 Hz was started 4 min before the addition of 15 μl of CS from a 30 μM stock on ice. Data collection was continued for 40 min.

2.7. Expression and purification of His-tagged p23 proteins

Plasmids encoding recombinant His-tagged p23 and p23-C18 was transformed into competent *E. coli* BL21 (DE3) (Stratagene, La Jolla, CA, USA). Expression was induced with 1 mM IPTG for 2 h at 37 °C. Lysates with 1 mg/ml lysozyme were prepared from the pelleted bacteria, and following a freeze–thaw cycle DNA and insoluble material were removed by centrifugation. HITrap Chelating HP 1 ml columns (Amersham Biosciences) loaded with $NiSO_4$ were used for purification of the His-tagged proteins. Elution was done with 500 mM imidazole in PBS. Fractions with His-tagged protein were pooled and dialysed against 40 mM HEPES–KOH, pH 7.5. The concentrations of purified His-p23-wt and His-p23-C18 were determined using the calculated absorption of 2.04 and 1.89 for a 1 mg/ml solution in a 1 cm cuvette at 280 nm, respectively.

3. Results

3.1. Cleavage of p23 during programmed cell death

Previously, we reported that activation of the Fas receptor by antibody cross-linking led to the cleavage of the hsp90 co-chaperone p23 in Jurkat-E6 cells [18]. To examine whether activation of other death receptors also leads to the cleavage of p23, NIH3T3 cells were stimulated with TNFα and CHX. Inhibition of translation by CHX prevents synthesis of the anti-apoptotic caspase-8 inhibitor $FLIP_L$, whose expression is stimulated following the activation of NFκB by TNFα [23]. Significant cleavage of p23 was observed in NIH3T3 cells after TNFα stimulation in the presence of CHX, whereas CHX or TNFα alone had no effect (Fig. 1(a)). Activation of the intrinsic death pathway in Jurkat-E6 cells by staurosporine (STS) resulted also in p23 cleavage (Fig. 1(b)). Furthermore, we have observed that p23 is cleaved in HeLa cells exposed to TNFα/CHX and in UV-exposed HUVEC cells (data not shown). These results demonstrate that p23 cleavage occurs independent on whether the extrinsic or the intrinsic death pathway is activated, indicating that the degradation of p23 may be a general hallmark of apoptosis.

3.2. p23 cleavage is prevented by caspase inhibitors

To verify whether caspases are responsible for the cleavage of p23, the broad range caspase inhibitor zVAD-fmk, or Ac-DEVD-CHO, an inhibitor of caspase-3 like activity, were added to Jurkat-E6 cells at the time of Fas receptor cross-linking. Both zVAD-fmk and Ac-DEVD-CHO prevented the cleavage of p23 in Jurkat-E6 cells, whereas p23 was processed as expected in the absence of these inhibitors (Fig. 2(a)). When the effect of zVAD-fmk and Ac-DEVD-CHO on TNFα/CHX induced apoptosis was examined in NIH3T3 cells, we also observed complete prevention of p23 cleavage by zVAD-fmk, while Ac-DEVD-CHO had no effect (Fig. 2(b)). This could indicate that different caspases are activated in Jurkat-E6 cells during Fas induced apoptosis as compared to TNFα/CHX induced apoptosis in NIH3T3 cells. However, it cannot be ruled out that the NIH3T3 cells are less sensitive to Ac-DEVD-CHO.

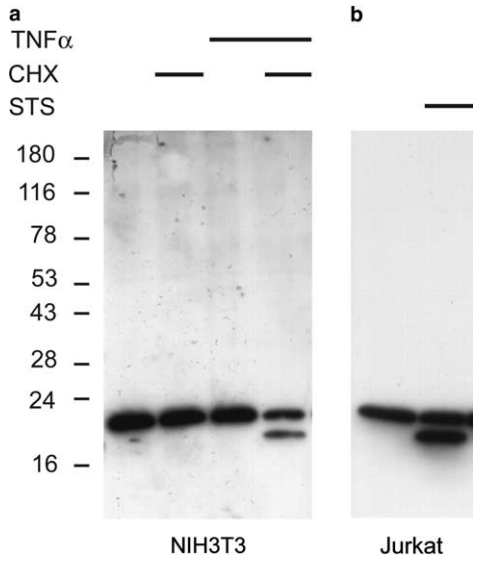

Fig. 1. p23 cleavage following TNFα/CHX or STS treatment. Immunoblotting of p23 from NIH3T3 (a) or Jurkat-E6 (b) cell lysates. NIH3T3 cells were incubated with 20 ng/ml TNFα and 10 μg/ml cycloheximide for 4 h, and Jurkat-E6 cells were incubated with 1 μM STS for 4 h. Proteins (10 μg) in the cell lysates were separated by SDS–PAGE. Following semi-dry transfer to a PVDF membrane, p23 immunoreactivity was developed using the p23 clone 22 antibody and a HRP-conjugated goat anti mouse IgG secondary antibody. Chemiluminescence signals were visualised using ECL and exposure to X-ray film. Equal gel loading was verified by Coomassie brilliant blue G staining of the membrane (not shown).

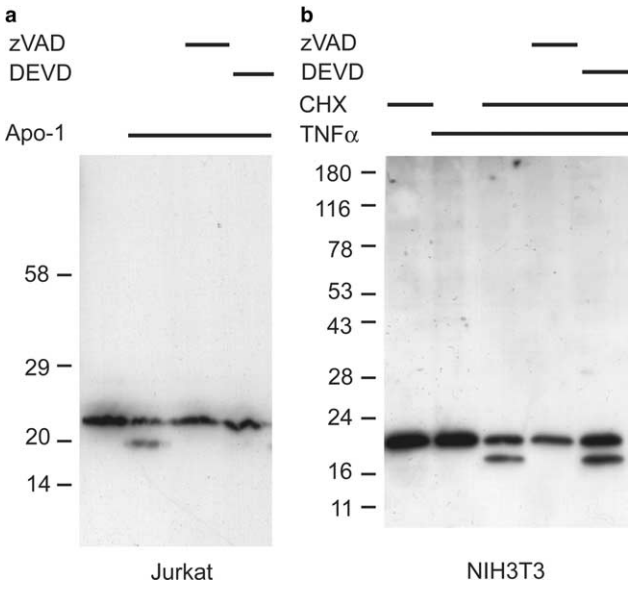

Fig. 2. Caspase inhibitors prevent p23 cleavage. p23 immunoblots of Jurkat-E6 (a) and NIH3T3 cell lysates (b). At the timepoint of Fas receptor crosslinking in Jurkat-E6 cells, or addition of 20 ng/ml TNFα and 10 μg/ml CHX to NIH3T3 cells, the caspase inhibitors zVAD-fmk (20 μM) or DEVD-CHO (30 μM) were added to the cells. After 4 h the cells were harvested. SDS–PAGE and immunoblotting of p23 was carried out as described in Fig. 1.

3.3. p23 is cleaved by recombinant caspase-3 and caspase-8 at Asp 142 in vitro

By tryptic in-gel digest of immunoprecipitated full length and truncated p23 followed by matrix assisted laser desorption ionisation time of flight (MALDI TOF) mass spectrometry, we obtained detailed information of the peptide composition and possible caspase cleavage sites in p23 [18]. Based on this information we predicted aspartic acids 142 and 150 as the likely cleavage sites. To test whether caspases are able to cleave p23 at these sites in vitro, we generated ^{35}S-methionine labelled p23 proteins by in vitro translation in which Asp 142 or Asp 150 were changed to Glu (D142E or D150E). The proteins were visualised by autoradiography and their identities verified by immunoblotting using the anti-p23 clone 22 antibody (data not shown). In the absence of the plasmid template, p23 was not detected in the extracts (data not shown). We incubated p23, p23-D142E or p23-D150E with purified active recombinant caspase-3 or caspase-8 and examined the cleavage of these proteins by autoradiography. p23 and p23-D150E were cleaved following a 1 h incubation with caspase-3 or caspase-8, whereas p23-D142E was left un-cleaved by both caspases (Fig. 3). These data provide strong evidence that p23 is cleaved within the PEVD^{142}G sequence after Asp 142 by caspase-3 and caspase-8 in vitro, whereas these caspases do not cleave p23 after Asp 150 within the DSQD^{150}S sequence.

3.4. GA sensitises p23 cleavage

To investigate whether blocking of the p23–hsp90 interaction by GA has any effect on the cleavage of p23 during apoptosis in NIH3T3 cells, we examined the effect of overnight incubation with 0.5 μM GA followed by TNFα/CHX treatment. Following the 18 h GA treatment we observed the truncated form of p23 in NIH3T3 cell lysates (Fig. 4(a)). GA treated NIH3T3 cells rapidly became apoptotic following addition of TNFα in the absence of CHX, as judged by morphological criteria (data not shown), and GA sensitised the cells to TNFα induced p23 cleavage in the absence of CHX (Fig. 4). The sensitisation of TNFα induced p23 cleavage by GA could be prevented by the co-addition of the caspase inhibitor zVAD-fmk (Fig. 4(a)). The data indicate that GA accelerates the demise of p23 in NIH3T3 cells and p23 seems to be partially protected from cleavage by the association with hsp90. However, we cannot rule out that the sensitisation of p23 cleavage by GA is indirectly caused by down-regulation and

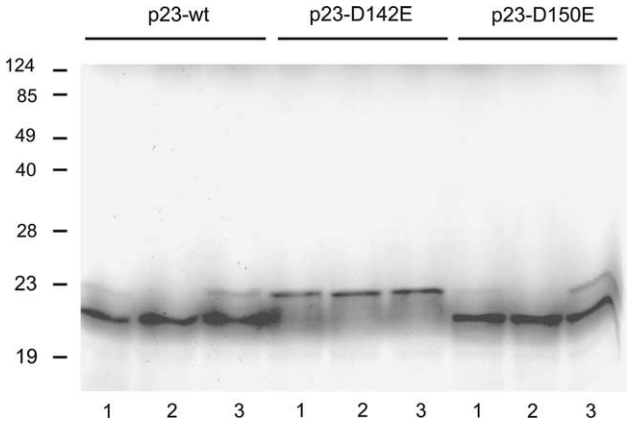

Fig. 3. Cleavage of in vitro synthesised p23 by recombinant caspase-3 and 8. Autoradiography of ^{35}S-methionine labelled p23-wt, p23-D142E, and p23-D150E after incubation at 37 °C for 1 h with 0.8 μM recombinant caspase-3 (lanes 1), 0.8 μM recombinant caspase-8 (lanes 2) or 0.2 μM recombinant caspase-8 (lanes 3).

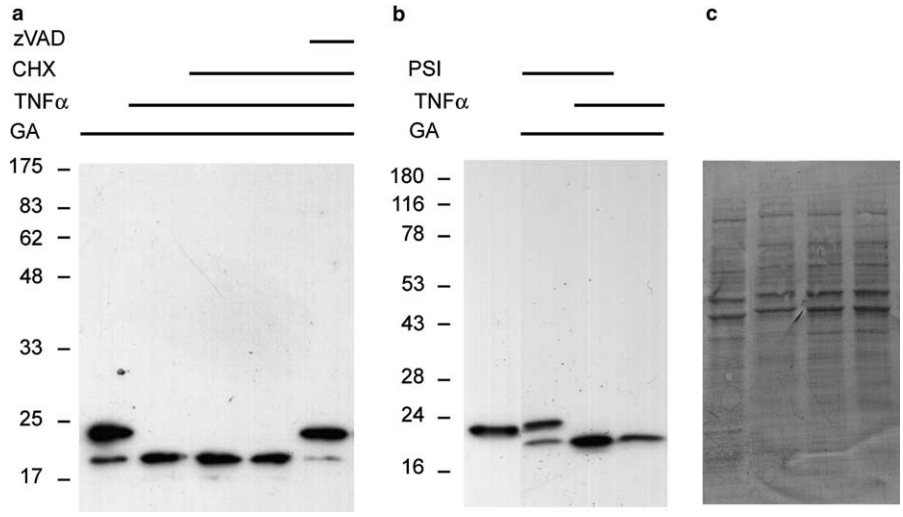

Fig. 4. GA accelerates p23 cleavage and PSI stabilises truncated p23. NIH3T3 cells were pre-incubated with 0.5 μM GA for 18 h, then TNFα (20 ng/ml in lane 3 and 50 ng/ml in lane 4), 10 μg/ml CHX, or 10 μM zVAD-fmk as indicated were added and the cells harvested after 4 h (a). NIH3T3 cells were pre-incubated with 0.5 μM GA for 18 h, then 20 μM PSI, or 20 ng/ml TNFα as indicated were added and the cells harvested after 4 h (b). SDS–PAGE and immunoblotting of p23 was carried out as described in Fig. 1. Coomassie brilliant blue G staining of the membrane in (b) is shown to visualise equal loading levels (c).

inactivation of the numerous hsp90 client proteins that are dependent on the hsp90 chaperone machinery.

3.5. *Proteasome inhibition does not prevent the initial p23 cleavage*

To rule out that full length p23 was cleaved by proteasome dependent proteolysis, we tested whether the potent inhibitor of the proteasomal chymotrypsin-like activity, carbobenzoxy-L-isoleucyl-γ-*t*-butyl-L-glutamyl-L-alanyl-L-leucinal (PSI) prevented the GA and TNFα induced cleavage of p23 in NIH3T3 cells. Cells treated with GA were exposed to TNFα, PSI or both. In cells treated with PSI only we did not observe cleavage of p23 (data not shown). Addition of PSI to the GA treated cells led to a minor accumulation of truncated p23 (Fig. 4(b)), indicating that PSI did not protect full length p23 from degradation but accelerated the caspase-mediated initial cleavage of p23. Combined treatment with TNFα, PSI and GA led to the complete disappearance of full-length p23 as did GA and TNFα treatment, but truncated p23 consistently accumulated to a greater extent in the GA, PSI and TNFα treated cells as compared to the GA and TNFα treated cells (Fig. 4(b)). In support of this conclusion the Coomassie brilliant blue G stained membrane is also shown to verify equal loading levels (Fig. 4(c)). The increased stability of truncated p23 in the presence of PSI indicates that truncated p23 is a substrate for chymotrypsin-like activity of the proteasome in NIH3T3 cells.

We also analysed the effect of PSI on the time course of p23 degradation in Jurkat-E6 cells following Fas receptor crosslinking. For this purpose Jurkat-E6 cells were induced to apoptosis in the presence or absence of PSI. Truncated p23 appeared at the same time point in the absence (Fig. 5(a)) or presence (Fig. 5(b)) of PSI, but full-length p23 disappeared faster in the presence of PSI. Importantly, the ratio of full-lenght p23 to truncated p23 is in strong favour of truncated p23 in the presence of PSI (Fig. 5). This observation support the suggestion that truncated p23 is degraded by the proteasome.

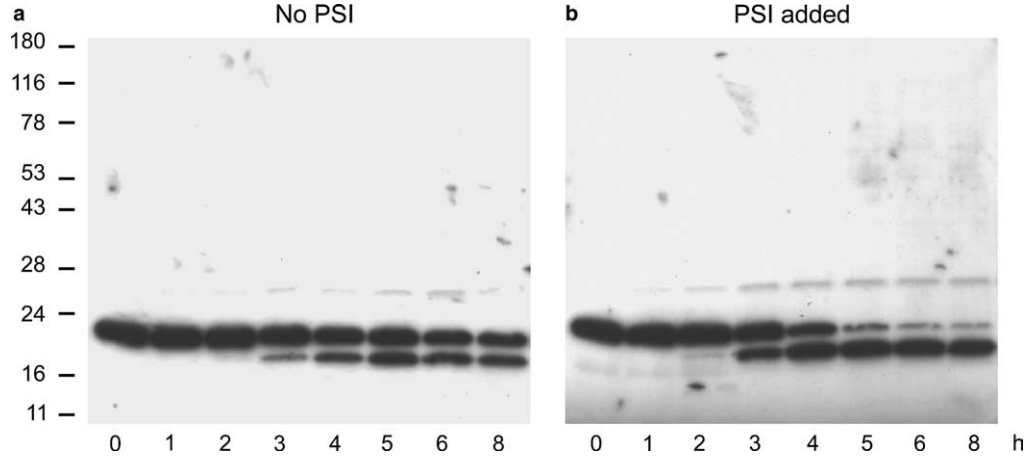

Fig. 5. PSI changes the ratio between p23 and truncated p23 in favour of truncated p23. Apoptosis was induced by Fas receptor crosslinking of Jurkat-E6 cells in the absence (a) or presence (b) of 20 μM PSI, and cell samples were harvested at different time points. SDS–PAGE and immunoblotting of p23 was carried out as described in Fig. 1.

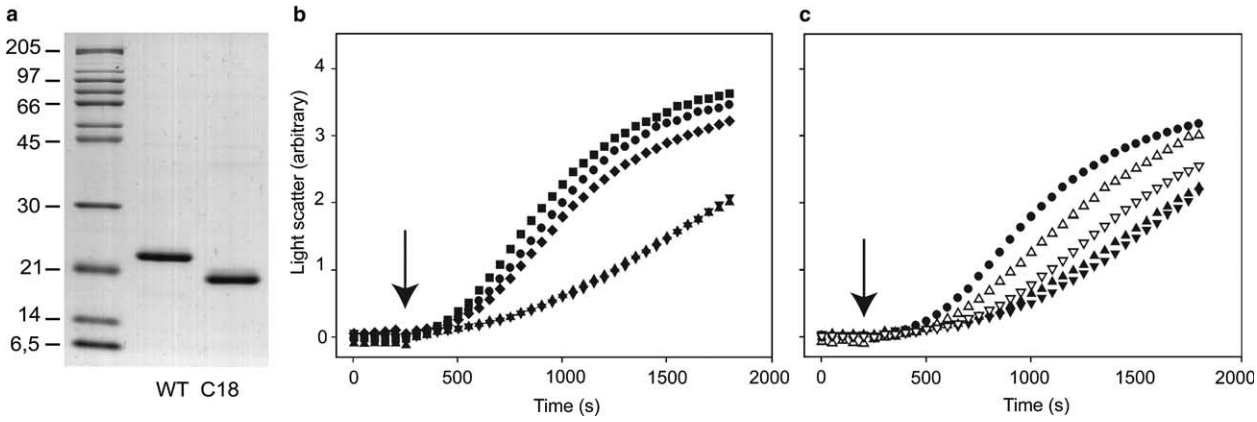

Fig. 6. Truncated p23 has passive chaperone activity. Purified His-tagged human p23 and His-tagged human p23-C18 (18 C-terminal aa deleted) were stained with Coomassie brilliant blue G (a). CS light scatter at 500 nm was recorded in the absence (circle) or presence of p23-wt (triangle down), p23-C18 (triangle up), BSA (square), or IgG (diamond) at a 2-fold molar excess to CS (b). CS light scatter at 500 nm was recorded in the absence (circle) or presence of p23-wt (triangle down) or p23-C18 (triangle up) at equal molar levels to CS (closed triangles) or at 2-fold molar excess (open triangles) of CS (c). The arrows in (b) and (c) indicate the time of CS addition to the cuvette.

3.6. Anti-aggregating effect of recombinant truncated p23

p23 has been proposed to be a chaperone on its own [11], as purified recombinant p23 delays the aggregation of heat inactivated CS [10,24]. Therefore, we tested whether cleavage of p23 in the C-terminal region that removes the 18 C-terminal aa could impair the anti-aggregating activity of the protein. Recombinant His-p23 and His-p23-C18, that resembles the caspase cleaved p23, were analysed by SDS–PAGE and Coomassie staining (Fig. 6(a)). We observed aggregation of 0.3 μM heat inactivated CS following incubation at 43 °C as expected, and BSA or rabbit purified IgG used as controls did not affect this aggregation of CS (Fig. 6(b)). In contrast, addition of His-p23 or His-p23-C18 greatly reduced the speed of CS aggregation (Fig. 6(b)), to the same extent as previously described [24]. We did not observe any difference in the anti-aggregating effect of the two proteins at a 1:2 molar ratio of CS to His-p23 or His-p23-C18 (Fig. 6(b)), and higher concentrations of His-tagged p23 did not change the slope of the curves (data not shown). However, when the amount of His-tagged p23 was decreased to a molar ratio of 2:1 (CS: His-p23 or His-p23-C18), His-p23-C18 was less effective in preventing CS aggregation when compared to the full length His-p23 (Fig. 6(c)). These data indicate that the anti-aggregating activity of p23 is diminished following removal of the 18 C-terminal residues, although the His-p23-C18 recombinant protein still has anti-aggregating activity that prevents the aggregation of heat inactivated CS, when present in excess.

4. Discussion

The data presented in this paper show that the hsp90 co-chaperone p23 is a target for caspases which are activated in apoptosis induced by either intrinsic or extrinsic pathways. The data also indicate that truncated p23 is a substrate for proteasomal degradation. The cleavage of p23 by caspases leaves a truncated p23 with reduced anti-aggregating activity. Other putative functional consequences of p23 cleavage and degradation may be a decline in the cellular PGE_2 synthesis, changed transcriptional regulation by steroid hormone receptors, and abolishment of hsp90 chaperone activity.

The degradation of p23 following activation of the intrinsic or extrinsic apoptotic pathways could be part of the elimination of the hsp90 chaperone machinery, accelerating the death process. Although speculative, this is in agreement with the reported protective function of the hsp90 chaperone complex during apoptosis [25]. Hsp90 was reported to repress caspase-dependent apoptosis via inhibition of the formation of a functional apoptosome through binding to Apaf-1, thereby preventing Apaf-1 oligomerisation.

Hsp90 was described to stabilise receptor interacting protein (RIP) which is recruited to activated TNFR-1, where RIP is needed for activation of NFκB and c-Jun N-terminal protein kinase upon TNFα signalling [26]. Targeting of the hsp90 chaperone by GA resulted in RIP degradation and subsequent increased vulnerability to cell death following TNFR-1 activation due to the abolished NFκB activation. Additionally, it was shown that destabilisation of RIP was prevented by proteasome inhibition but not by caspase inhibition.

We have observed that GA sensitises NIH3T3 cells to TNFα-induced apoptosis. In addition, we and others [19] found that GA accelerates caspase-dependent p23 cleavage, and therefore RIP and p23 do not seem to be degraded by similar routes. NIH3T3 cells over-expressing hsp90 were shown to partially suppress caspase-3 activation and combined TNFα/CHX-induced apoptosis [27]. Since the hsp90 chaperone activity is dependent on p23, our observations indicate that targeting of p23 by caspases and the proteasome, is one likely route leading to the inactivation of the hsp90 chaperone complex. Indeed, inhibition of the hsp90 chaperone has been shown to alter the delicate balance between cell survival and death towards the latter, as is seen after long term GA treatment of tumour cells. Up-regulation of p23 in tumour cells [16,18] to increase the activity of hsp90, may be a survival strategy of cancer cells.

The cleavage of p23 at Asp 142 during apoptosis leaves a truncated p23 with the ultimate C-terminal sequence PEVD. The recognition motif on hsp70 and hsp90 for tetratricopeptide repeat (TPR) domain containing proteins is a C-terminal EEVD sequence. The initial cleavage of p23 during apoptosis therefore leaves a truncated p23 that may interfere with the binding of TPR domain containing proteins to hsp90 or hsp70.

It has been reported that hsp90 directs client proteins to degradation by the proteasome [28], but the molecular events that convert hsp90 from a chaperone to a complex facilitating client protein degradation is unknown. The carboxy terminus of hsc70 interacting protein (CHIP) that binds hsp90 is an E3 ubiquitin ligase. CHIP interact with the C-terminal part of hsp90 through its TPR and the adjacent charged domain. CHIP has been shown to take part in protein quality control that carry out selective ubiquitination of target proteins in their non-native state when these client proteins are "assisted" by the chaperone complex [29]. The ubiquitination of client proteins bound to the C-terminal chaperone site of hsp90 by CHIP, results in their subsequent degradation by the proteasome. Interestingly, the association of CHIP with the hsp90 chaperone complex has been shown to result in dissociation of p23 from the complex [30], because p23 and CHIP compete for binding to hsp90 even though their binding sites are different. Therefore, the presence of p23 in non-apoptotic cells prevents CHIP from associating with hsp90, whereas, p23 degradation during apoptosis could facilitate the CHIP–hsp90 interaction. The hsp90 chaperone activity is thereby shifted into a CHIP complex facilitating proteasomal degradation of client proteins. This may suggest that p23 plays a role of a caspase-sensitive switch that enables targeted disruption of hsp90 client proteins during apoptosis.

Acknowledgements: We thank Ulla Mortensen for technical assistance and Svetlana Tarabykina for critically reading of this manuscript. This work was supported by grants from the Danish Cancer Society (20-50327), the Danish Natural Science Research Council (24-56881), and The Lundbeck Foundation (20-506400-57308) to MWB.

References

[1] Lai, B.T., Chin, N.W., Stanek, A.E., Keh, W. and Lanks, K.W. (1984) Quantitation and intracellular localization of the 85 K heat shock protein by using monoclonal and polyclonal antibodies. Mol. Cell. Biol. 4, 2802–2810.
[2] Smith, D.F., Whitesell, L., Nair, S.C., Chen, S., Prapapanich, V. and Rimerman, R.A. (1995) Progesterone receptor structure and function altered by geldanamycin, an hsp90-binding agent. Mol. Cell. Biol. 15, 6804–6812.
[3] Felts, S.J. and Toft, D.O. (2003) p23, a simple protein with complex activities. Cell Stress Chaperones 8, 108–113.
[4] Young, J.C. and Hartl, F.U. (2000) Polypeptide release by Hsp90 involves ATP hydrolysis and is enhanced by the co-chaperone p23. EMBO J. 19, 5930–5940.
[5] Workman, P. (2003) Overview: translating Hsp90 biology into Hsp90 drugs. Curr. Cancer Drug Targets 3, 297–300.
[6] Roe, S.M., Prodromou, C., O'Brien, R., Ladbury, J.E., Piper, P.W. and Pearl, L.H. (1999) Structural basis for inhibition of the Hsp90 molecular chaperone by the antitumor antibiotics radicicol and geldanamycin. J. Med. Chem. 42, 260–266.
[7] Sullivan, W., Stensgard, B., Caucutt, G., Bartha, B., McMahon, N., Alnemri, E.S., Litwack, G. and Toft, D. (1997) Nucleotides and two functional states of hsp90. J. Biol. Chem. 272, 8007–8012.
[8] Sullivan, W.P., Owen, B.A. and Toft, D.O. (2002) The influence of ATP and p23 on the conformation of hsp90. J. Biol. Chem. 277, 45942–45948.
[9] Morishima, Y., Kanelakis, K.C., Murphy, P.J., Lowe, E.R., Jenkins, G.J., Osawa, Y., Sunahara, R.K. and Pratt, W.B. (2003) The hsp90 cochaperone p23 is the limiting component of the multiprotein hsp90/hsp70-based chaperone system in vivo where it acts to stabilize the client protein: hsp90 complex. J. Biol. Chem. 278, 48754–48763.
[10] Bose, S., Weikl, T., Bugl, H. and Buchner, J. (1996) Chaperone function of Hsp90-associated proteins. Science 274, 1715–1717.
[11] Freeman, B.C., Toft, D.O. and Morimoto, R.I. (1996) Molecular chaperone machines: chaperone activities of the cyclophilin Cyp-40 and the steroid aporeceptor-associated protein p23. Science 274, 1718–1720.
[12] Freeman, B.C., Felts, S.J., Toft, D.O. and Yamamoto, K.R. (2000) The p23 molecular chaperones act at a late step in intracellular receptor action to differentially affect ligand efficacies. Genes Dev. 14, 422–434.
[13] Freeman, B.C. and Yamamoto, K.R. (2002) Disassembly of transcriptional regulatory complexes by molecular chaperones. Science 296, 2232–2235.
[14] Li, W., Jin, K., Nagayama, T., He, X., Chang, J., Minami, M., Graham, S.H., Simon, R.P. and Greenberg, D.A. (2000) Increased expression of apoptosis-linked gene 2 (ALG2) in the rat brain after temporary focal cerebral ischemia. Neuroscience 96, 161–168.
[15] Krebs, J. and Klemenz, R. (2000) The ALG-2/AIP-complex, a modulator at the interface between cell proliferation and cell death? A hypothesis. Biochim. Biophys. Acta 1498, 153–161.
[16] Krebs, J., Saremaslani, P. and Caduff, R. (2002) ALG-2: a Ca^{2+}-binding modulator protein involved in cell proliferation and in cell death. Biochim. Biophys. Acta 1600, 68–73.
[17] Martinet, W., Schrijvers, D.M., De Meyer, G.R.Y., Herman, A.G. and Kockx, M.M. (2003) Western array analysis of human atherosclerotic plaques: downregulation of apoptosis-linked gene 2. Cardiovasc. Res. 60, 259–267.
[18] Mollerup, J., Krogh, T.N., Nielsen, P.F. and Berchtold, M.W. (2003) Properties of the co-chaperone protein p23 erroneously attributed to ALG-2 (apoptosis-linked gene 2). FEBS Lett. 555, 478–482.
[19] Gausdal, G., Gjertsen, B.T., Fladmark, K.E., Demol, H., Vandekerckhove, J. and Doskeland, S.O. (2004) Caspase-dependent, geldanamycin-enhanced cleavage of co-chaperone p23 in leukemic apoptosis. Leukemia 18, 1989–1996.
[20] Dhein, J., Daniel, P.T., Trauth, B.C., Oehm, A., Moller, P. and Krammer, P.H. (1992) Induction of apoptosis by monoclonal antibody anti-APO-1 class switch variants is dependent on cross-linking of APO-1 cell surface antigens. J. Immunol. 149, 3166–3173.
[21] Sawano, A. and Miyawaki, A. (2000) Directed evolution of green fluorescent protein by a new versatile PCR strategy for site-directed and semi-random mutagenesis. Nucleic Acids Res. 28, E78.
[22] Buchner, J., Grallert, H. and Jakob, U. (1998) Analysis of chaperone function using citrate synthase as nonnative substrate protein. Methods Enzymol. 290, 323–338.
[23] Micheau, O., Lens, S., Gaide, O., Alevizopoulos, K. and Tschopp, J. (2001) NF-kappaB signals induce the expression of c-FLIP. Mol. Cell Biol. 21, 5299–5305.
[24] Weikl, T., Abelmann, K. and Buchner, J. (1999) An unstructured C-terminal region of the Hsp90 co-chaperone p23 is important for its chaperone function. J. Mol. Biol. 293, 685–691.
[25] Pandey, P., Saleh, A., Nakazawa, A., Kumar, S., Srinivasula, S.M., Kumar, V., Weichselbaum, R., Nalin, C., Alnemri, E.S., Kufe, D. and Kharbanda, S. (2000) Negative regulation of cytochrome *c*-mediated oligomerization of Apaf-1 and activation of procaspase-9 by heat shock protein 90. EMBO J. 19, 4310–4322.
[26] Lewis, J., Devin, A., Miller, A., Lin, Y., Rodriguez, Y., Neckers, L. and Liu, Z.G. (2000) Disruption of hsp90 function results in degradation of the death domain kinase, receptor-interacting protein (RIP), and blockage of tumor necrosis factor-induced nuclear factor-kappaB activation. J. Biol. Chem. 275, 10519–10526.
[27] Zhao, C. and Wang, E. (2004) Heat shock protein 90 suppresses tumor necrosis factor alpha induced apoptosis by preventing the cleavage of Bid in NIH3T3 fibroblasts. Cell Signal. 16, 313–321.
[28] Ballinger, C.A., Connell, P., Wu, Y., Hu, Z., Thompson, L.J., Yin, L.Y. and Patterson, C. (1999) Identification of CHIP, a novel tetratricopeptide repeat-containing protein that interacts with heat shock proteins and negatively regulates chaperone functions. Mol. Cell. Biol. 19, 4535–4545.
[29] Murata, S., Chiba, T. and Tanaka, K. (2003) CHIP: a quality-control E3 ligase collaborating with molecular chaperones. Int. J. Biochem. Cell Biol. 35, 572–578.
[30] Connell, P., Ballinger, C.A., Jiang, J., Wu, Y., Thompson, L.J., Hohfeld, J. and Patterson, C. (2001) The co-chaperone CHIP regulates protein triage decisions mediated by heat-shock proteins. Nat. Cell Biol. 3, 93–96.